Interferometry of hyper-Rayleigh scattering by inhomogeneous thin films

A.A. Fedyanin, N.V. Didenko, N.E. Sherstyuk, A.A. Nikulin, O.A. Aktsipetrov*

Department of Physics, Moscow State University, Moscow 119899, Russia

February 2, 2008

Abstract

The use of specific symmetry properties of the optical second-harmonic generation (the s,s-exclusion rule) has allowed us to observe high-contrast hyper-Rayleigh interference patterns in a completely diffuse light - an effect having no analog in case of linear (Rayleigh) scattering.

*E-mail address: aktsip@astral.ilc.msu.su, Web: http://kali.ilc.msu.su

In the past few years the versatility of optical second-harmonic generation (SHG)[1] as a probe for studying solid state nanostructures and low-dimensional systems has been embodied in experimental methods of SHG interferometry (phase measurements)[2] and hyper-Rayleigh scattering (HRS)[3]. These methods exploit opposite features of the second-harmonic (SH) radiation generated by an object being studied: the former implies coherence of the SH radiation, whereas the latter deals with incoherent SHG originating from spatial fluctuations of the optical parameters in a randomly inhomogeneous system. Therefore the very idea of the HRS interferometry may seem contradictory, which is, however, disproved by a more detailed analysis of a conventional experimental scheme of SHG interferometry. In this scheme shown in Fig. 1, panel 1, the interference pattern is formed by the SH wave from a sample studied and that from another object having well-defined optical characteristics and used as a reference. The phase shift between the two waves results from the dispersion of the refraction index of air n, which yields the following dependence of the total SHG intensity $I_{2\omega}$ on the reference translation:

$$I_{2\omega}(x_{\mathrm{R}}) = I_{2\omega}^{\mathrm{S}} + I_{2\omega}^{\mathrm{R}} + 2\alpha\sqrt{I_{2\omega}^{\mathrm{S}} I_{2\omega}^{\mathrm{R}}}\cos\left[\Phi_0 + K(x_{\mathrm{R}} - x_{\mathrm{S}})\right], \tag{1}$$

where $I_{2\omega}^{\mathrm{S}}$ and $I_{2\omega}^{\mathrm{R}}$ are the intensities of the SH waves from the sample and the reference, respectively, α is the mutual coherence factor of the two waves, x_{S} and x_{R} are the coordinates of the sample and the reference, respectively, measured in the reference translation direction, Φ_0 is position-independent part of the relative phase shift between the two waves, $K = 2\omega(n(2\omega) - n(\omega))/c$ and ω is the fundamental radiation frequency. The essential point is that the SH wave from the reference is then reflected from the sample. It is the feature of the interferometry scheme that allows us to observe HRS interference patterns. A randomly inhomogeneous sample is a source of both HRS of the fundamental radiation and Rayleigh scattering (RS) of the SH wave generated by the reference and then linearly reflected by the sample. In other words, the SH wave from the reference, after being reflected from the sample, becomes 'modulated' by the spatial fluctuations of the linear-optical properties of the sample. Therefore the interfering SH fields from the reference and the sample will both

have incoherent components that are *mutually* coherent (statistically dependent) because of their common statistical origin: the spatial fluctuations of the optical parameters of the sample. This modifies Eq.(1) for the resulting interference pattern as follows:

$$I_{2\omega}(x_{\mathrm{R}}) = I_{2\omega}^{\mathrm{S}} + I_{2\omega}^{\mathrm{R}} + 2\bar{\alpha}\sqrt{\bar{I}_{2\omega}^{\mathrm{S}}\bar{I}_{2\omega}^{\mathrm{R}}}\cos[\bar{\Phi} + Kx_{\mathrm{R}}] + 2\tilde{\alpha}\sqrt{\tilde{I}_{2\omega}^{\mathrm{S}}\tilde{I}_{2\omega}^{\mathrm{R}}}\cos[\tilde{\Phi} + Kx_{\mathrm{R}}], \qquad (2)$$

where $I_{2\omega}^{\mathrm{S}} = \bar{I}_{2\omega}^{\mathrm{S}} + \tilde{I}_{2\omega}^{\mathrm{S}}$, $I_{2\omega}^{\mathrm{R}} = \bar{I}_{2\omega}^{\mathrm{R}} + \tilde{I}_{2\omega}^{\mathrm{R}}$ and the bar (tilde) over a quantity denotes a coherent (incoherent) component. For the *s*-in,*s*-out wave-polarization combination the coherent component $\bar{I}_{2\omega}^{\mathrm{S}}$ vanishes due to the *s,s*-exclusion rule[4], and solely an HRS interference pattern is observed.

In this paper we study two types of inhomogeneous solid films: those of purple membranes of bacteriorhodopsin (bR) and polycrystalline $\mathrm{Pb_x(Zr_{0.53}Ti_{0.47})O_3}$ (PZT) ferroelectric films. bR films with a thickness of about 1000 nm were prepared by the method described in Ref. [[5]]. PZT texture films were fabricated by the sol-gel technique[6] and then annealed at 650^0C. For SHG experiments the output of a Q - switched YAG:Nd^{3+} laser at 1064 nm is used as a fundamental radiation with the pulse duration, repetiton rate and intensity being 15 ns, 12.5 Hz and 1 MW/cm^2, respectively The *s*-polarized fundamental wave irradiates the sample at an angle of incidence $\theta_0 = 45^0$. Having passed through a set of color filters, the *s*-polarized SH component is then detected by a PMT. The interference patterns $I_{2\omega}(x_{\mathrm{R}})$ are obtained by translating the reference along the laser beam. The reference is a 2 mm-thick plate of fused quartz coated by a 30 nm-thick indium-tin oxide film. Declining the reference by $(0\div5)^0$ from the position perpendicular to the laser beam (see panel 1 in Fig. 1) affects $I_{2\omega}^{\mathrm{R}}$ but not the intensity of the fundamental radiation transmitted through the reference. This allows us to balance the values of $I_{2\omega}^{\mathrm{S}}$ and $I_{2\omega}^{\mathrm{R}}$ and thus to provide a maximal interference-pattern contrast attained at $I_{2\omega}^{\mathrm{S}} \approx I_{2\omega}^{\mathrm{R}}$. The values of $I_{2\omega}^{\mathrm{S}}$ and $I_{2\omega}^{\mathrm{R}}$ are measured separately by inserting an appropriate filter (infrared or green, respectively) in between the reference and sample. Fig. 1 shows the interference patterns for bR (panel 2) and PZT (panel 3) films. Well-pronounced oscillations of the total SHG intensity are observed.

Three additional optical experiments are performed for more thorough interpretation of

the HRS interferometry data. First, the dependences of the SH intensity $I_{2\omega}$ on the azimuthal angle ψ of the sample rotation about the axis normal to the film plane were measured and are presented in insets in Figs. 2, 3. For the bR film the dependence $I_{2\omega}(\psi)$ is practically isotropic within the error bars, whereas for the PZT film a pronounced anisotropy with one-fold symmetry occurs[7]. The interference pattern shown in Fig. 1, panel 3 was measured in the minimum of this dependence. Second, the dependences of the SH intensity on the polar scattering angle θ (HRS indicatrix) were measured and are shown in Figs. 2, 3. For both types of films the HRS indicatrices have maxima at $\theta = \theta_0$, but no SH signal jump is observed in the vicinity of the specular direction. This proves the absence of the regular SHG contribution in the specular direction for the s-in, s-out polarization combination at the values of the azumuthal angle chosen for the HRS interferometry measurements. Third, linear, or Rayleigh, scattering indicatrices were measured at the SH wavelength and are shown in Figs. 2, 3. The RS indicatrices, in contrast with the HRS ones, have sharp specular peaks corresponding to the coherent reflection of light.

Both the HRS indicatrix and that of RS with the coherent-reflection peak subtracted can be approximated by a superposition of two Gaussian peaks:

$$I_\sigma(\theta) = I_\sigma T(\theta) \left(\exp\left\{ -\left[k(\theta) l_\sigma\right]^2 \right\} + \gamma_\sigma \exp\left\{ -\left[k(\theta) L_\sigma\right]^2 \right\} \right), \tag{3}$$

where $k(\theta) = 2\omega\left(\sin\theta - \sin\theta_0\right)/c$, $\sigma = 1,\ 2$, the subscripts 1 and 2 denote the RS and HRS indicatrices, respectively, $T(\theta)$ is a known function being the transmission coefficient of the film-air interface at the SH wavelength with the dielectric constant of the film as an adjustable parameter, I_σ, γ_σ, l_σ, L_σ are adjustable parameters. The quantities l_σ and L_σ are correlation lengths characterizing the in-plane scales of spatial fluctuations of optical parameters in the films. The fitting to the experimental data yields $l_1^{\rm bR} \simeq l_2^{\rm bR} \simeq 200$ nm, $L_1^{\rm bR} \simeq L_2^{\rm bR} \simeq 1000$ nm, $l_1^{\rm PZT} \simeq l_2^{\rm PZT} \simeq 170$ nm, $L_1^{\rm PZT} \simeq L_2^{\rm PZT} \simeq 2000$ nm. Thus, for each film type RS and HRS have two common fluctuating sources that are statistically independent and characterized by Gaussian correlation functions with quite different correlation lengths l and L. One of the sources is likely to be the inhomogeneities in bR and PZT films:

membrane aggregates and microcrystallites, respectively. The other one presumably is the film interfacial roughness.

Since the interference patterns are measured under conditions that provide vanishing of the coherent SH signal from the sample, Eq.(2) takes the form:

$$I_{2\omega}^{s-s}(x_{\rm R}) = \widetilde{I}_{2\omega}^{\rm S} + I_{2\omega}^{\rm R} + 2\widetilde{\alpha}\sqrt{\widetilde{I}_{2\omega}^{\rm S}\widetilde{I}_{2\omega}^{\rm R}}\cos[Kx_{\rm R} + \widetilde{\Phi}], \tag{4}$$

where $\widetilde{I}_{2\omega}^{\rm S}$ and $I_{2\omega}^{\rm R}$ are measured quantities, $\widetilde{\alpha}$ is an adjustable parameter and $\widetilde{I}_{2\omega}^{\rm R} = I_1(\theta_0)$ is the value estimated from the maximun of RS indicatrix. In order to elucidate the statistical meaning of $\widetilde{\alpha}$ we relate $\widetilde{I}_{2\omega}^{\rm R}$ and $\widetilde{I}_{2\omega}^{\rm S}$ to the constituents of the polarization induced in the sample: $\widetilde{I}_{2\omega}^{\rm S} \propto \langle|\widetilde{\mathbf{P}}_{2\omega}^{\rm S}|^2\rangle$, $\widetilde{I}_{2\omega}^{\rm R} \propto \langle|\widetilde{\mathbf{P}}_{2\omega}^{R}|^2\rangle$. Here $\widetilde{\mathbf{P}}_{2\omega}^{\rm S}$ is the total polarization (i.e. the sum of quadratic and linear polarizations) induced in the sample at the SH frequency by the fundamental radiation, $\widetilde{\mathbf{P}}_{2\omega}^{\rm R} = \mathbf{P}_{2\omega}^{\rm R} - \langle\mathbf{P}_{2\omega}^{\rm R}\rangle$, $\mathbf{P}_{2\omega}^{\rm R}$ is the linear polarization induced in the sample upon reflection of the SH wave generated by the reference, and angular brackets denote averaging over spatial fluctuations. Hence $\widetilde{\alpha}$ is defined as follows:

$$\widetilde{\alpha} = {\rm Re}\langle(\widetilde{\mathbf{P}}_{2\omega}^{\rm R})^* \cdot \widetilde{\mathbf{P}}_{2\omega}^{\rm S}\rangle/\sqrt{\langle|\widetilde{\mathbf{P}}_{2\omega}^{\rm R}|^2\rangle\langle|\widetilde{\mathbf{P}}_{2\omega}^{\rm S}|^2\rangle}. \tag{5}$$

Thus the key point of our explanation of the mutual coherence occurring for the SH wave from reference and the diffuse SH signal from the sample is the fact that the SH radiation from the reference is subsequently reflected from the sample, which leads to statistical dependence of the signals.

According to the data on the RS and HRS indicatrices for both bR and PZT films, each HRS interference pattern can be decomposed into superposition of two interference patterns originating from the two statistically independent sources with correlation lengths l and L. Taking into account that, according to Eq.(3), $\widetilde{I}_{2\omega}^{\rm R} = I_1(\theta_0) = I_1\,(1+\gamma_1)$, $\widetilde{I}_{2\omega}^{\rm S} = I_2(\theta_0) = I_2\,(1+\gamma_2)$, we re-write Eq. (4) as follows:

$$I_{2\omega}^{s-s}(x_{\rm R}) = \overline{I}_{2\omega}^{\rm R} + I_1\,(1+\gamma_1) + I_2\,(1+\gamma_2) + 2a\sqrt{I_1 I_2}\left(\cos[Kx_{\rm R} + \widetilde{\Phi}_l] + \sqrt{\gamma_1\gamma_2}\cos[Kx_{\rm R} + \widetilde{\Phi}_L]\right), \tag{6}$$

where $0 \leq a \leq 1$, the parameters $I_{1,2}$ and $\gamma_{1,2}$ have the same values as in Eq. (3), whereas the parameters a, $\widetilde{\Phi}_l$ and $\widetilde{\Phi}_L$ are treated as adjustable ones. The phenomenological parameter a is introduced to take into account all external factors (such as incomplete coherence of the fundamental radiation) that reduce mutual coherence of the HRS and RS signals. Fitting the experimental data for interference patterns with Eq. (6), we obtain $a^{\mathrm{bR}} = 0.91$, $a^{\mathrm{PZT}} = 0.89$, $\widetilde{\Phi}_l^{\mathrm{bR}} - \widetilde{\Phi}_L^{\mathrm{bR}} = 1.7$ rad and $\widetilde{\Phi}_l^{\mathrm{PZT}} - \widetilde{\Phi}_L^{\mathrm{PZT}} = 3.1$ rad.

To summarize, interferometry of incoherent second-harmonic generation, or hyper-Rayleigh scattering, by inhomogeneous films of bacteriorhodopsin and ferroelectric ceramics has been carried out. High-contrast interference patterns are observed. This is interpreted as a result of mutual coherence of the second-harmonic radiation from the film proper and the reference second-harmonic wave incoherently reflected by the film.

We are thankful to A.S. Sigov, E.D. Mishina for fruitful discussions, K.A. Vorotilov for preparing PZT samples, and E.P. Lukashev for preparing bR samples. This work was supported by RFBR grants 97-02-17919, 97-02-17923, 96-15-96420 and 96-15-96476, INTAS-93 grant 0370(ext), INTAS-RFBR-95 grant 722, INTAS grant YSF-9, ISSEP grant d98-701, Programs "Center of Fundamental Optics and Spectroscopy" and "Universities of Russia" grant 1412.

REFERENCES

1. Y.R. Shen, Annu. Rev. Mater. Sci. **16**, 69 (1986); T.F. Heinz, in *Nonlinear surface electromagnetic phenomena*, H.-E. Ponath and G. I. Stegeman, eds., (North-Holland, Amsterdam, 1991), p. 355; J.F. McGilp, Prog. Surf. Sci. **49**, 1 (1995).

2. R.K. Chang, J. Ducuing, N. Bloembergen, Phys. Rev. Lett. **15**, 6 (1965); K. Kemnitz, K. Bhattacharyya, J.M. Hicks, G.R. Pinto, K.B. Eisenthal, T.F. Heinz, Chem. Phys. Lett. **131**, 285 (1986); R. Stolle, G. Marowsky, E. Schwarzberg, G. Berkovic, Appl. Phys. B **63**, 491 (1996).

3. K. Clays and A. Persoons, Phys. Rev. Lett. **66**, 2980 (1991); P.K. Schmidt, G.W. Rayfield, Appl. Opt. **33**, 4286 (1994); O.A. Aktsipetrov, A.A. Fedyanin, T.V. Murzina, G.P. Borisevich, A.A. Kononenko, J. Opt. Soc. Am. B **14**, 771 (1997); E.D. Mishina *et al.*, Surf. Sci. **382**, L696 (1997).

4. O.A. Aktsipetrov, N.N. Akhmediev, I.M. Baranova, E.D. Mishina, and V.R. Novak, Zh. Eksp. Teor. Fiz. **89**, 911 (1985) (Sov. Phys. JETP **62**, 524 (1985)); O. Keller, J. Opt. Am. B **2**, 367 (1985).

5. G. Varo, Acta Biol. Acad. Sci. Hung. **32**, 301 (1981).

6. K.A. Vorotilov, M.I. Yanovskaya, and O.A. Dorokhova, Integrated Ferroelectrics **3**, 33 (1993)

7. O.A. Aktsipetrov *et al.*, Ferroelectrics **183**, 215 (1996).

FIGURES

Fig. 1. Panel 1: the schematic of HRS interferometry. Panels 2 and 3: SHG interference patterns measured in the s-in, s-out wave-polarization combination and in the absence of the specular SH component for bR and PZT films, respectively. Solid curves: the dependences given by by Eq.(4) with $\widetilde{\alpha}^{\mathrm{bR}}$=0.51, $\widetilde{\alpha}^{\mathrm{PZT}}$=0.73. Dashed curves: partial interference patterns, referred to as patterns "l" and "L", from the RS/HRS sources with the correlation lengths l and L, respectively. The inset: the schematic of the pattern formation.

Fig. 2. RS (open circles) and HRS (solid circles) indicatrices for bR film. Solid curves: the dependences given by Eq.(3) with $\gamma_1^{\mathrm{bR}} = 3.0$, $\gamma_2^{\mathrm{bR}} = 0.34$. Dashed lines show characteristic levels of HRS and RS intensities. The inset: the SHG azimuthal dependence and its approximation by the zeroth Fourier component.

Fig. 3. RS (open circles) and HRS (solid circles) indicatrices for PZT film. Solid curves: the dependences given by Eq.(3) with $\gamma_1^{\mathrm{PZT}} = 293.0$, $\gamma_2^{\mathrm{PZT}} = 2.9$. Dashed lines show characteristic levels of HRS and RS intensities. Left inset: the SHG azimuthal dependence and its approximation by first two Fourier components. An arrow indicates the angle ψ_0 at which the SHG interference patterns are measured. Right inset: the RS indicatrix in the logarithmic scale.

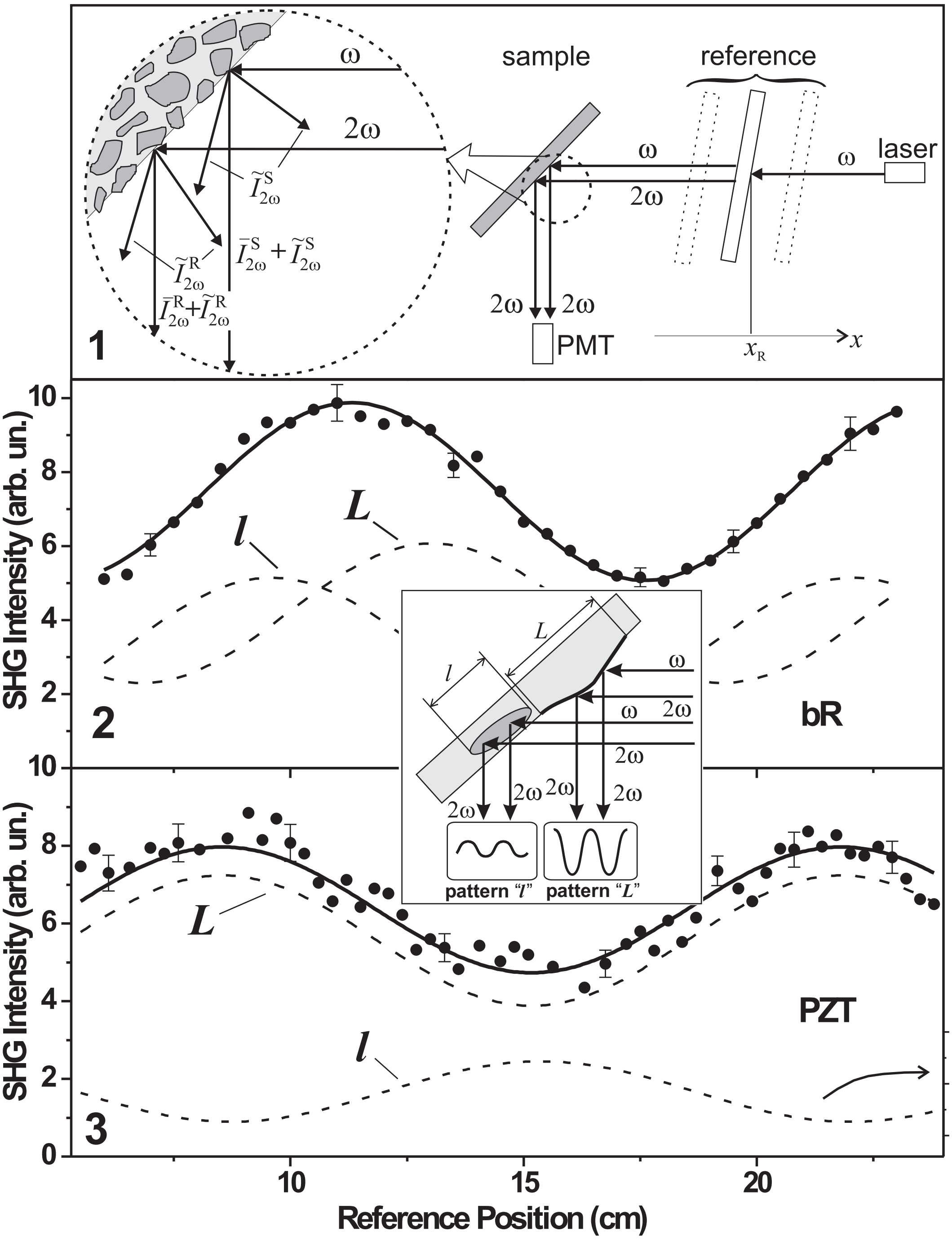

1
ω
2ω
sample
reference
laser
PMT
x
2
SHG Intensity (arb. un.)
L
l
bR
pattern "l"
pattern "L"
3
PZT
Reference Position (cm)

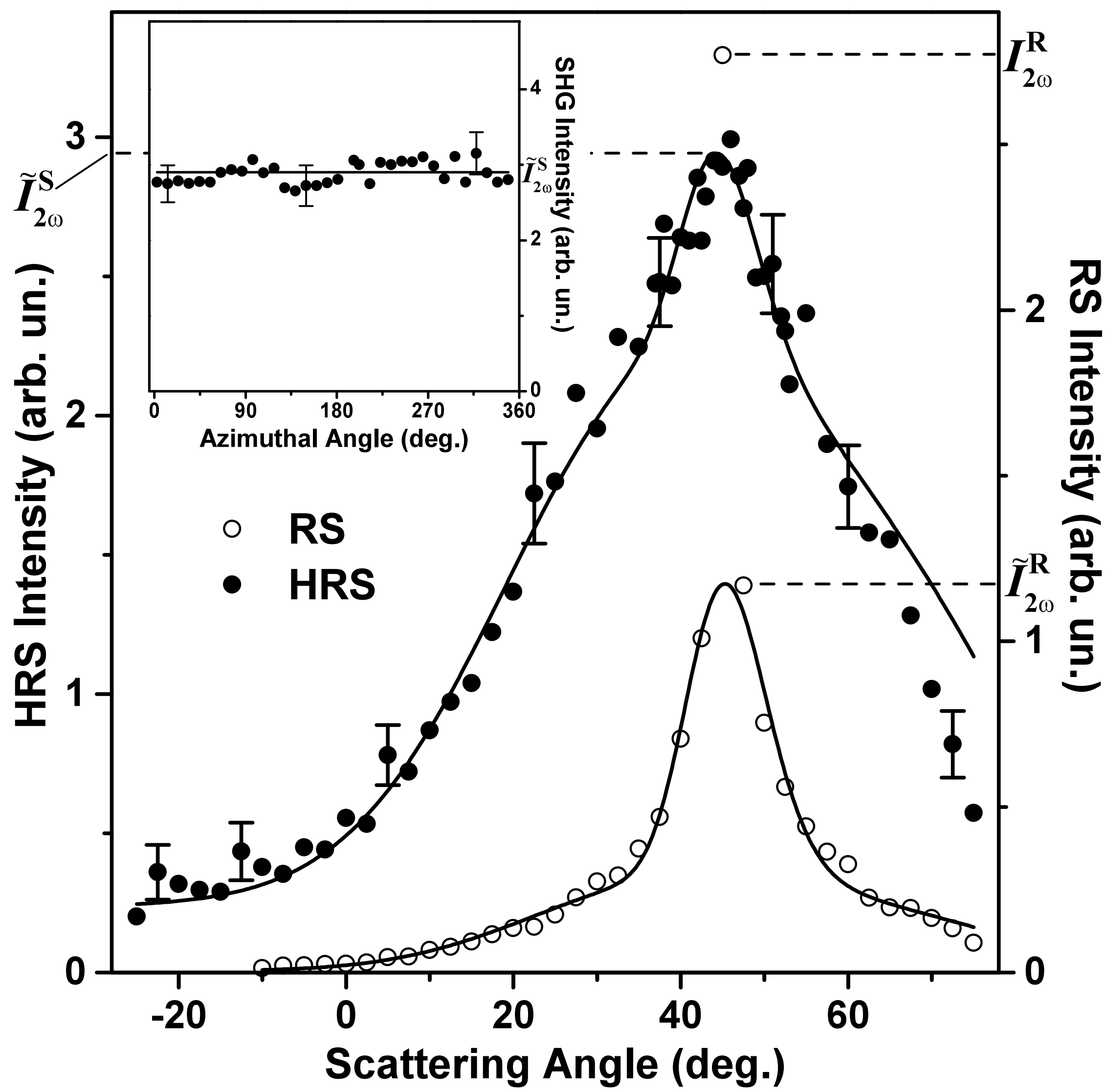

HRS Intensity (arb. un.)
RS Intensity (arb. un.)
Scattering Angle (deg.)
RS
HRS
$I^{R}_{2\omega}$
$\tilde{I}^{R}_{2\omega}$
$\tilde{I}^{S}_{2\omega}$
SHG Intensity (arb. un.)
Azimuthal Angle (deg.)
0
1
2
3
-20
0
20
40
60
4
90
180
270
360

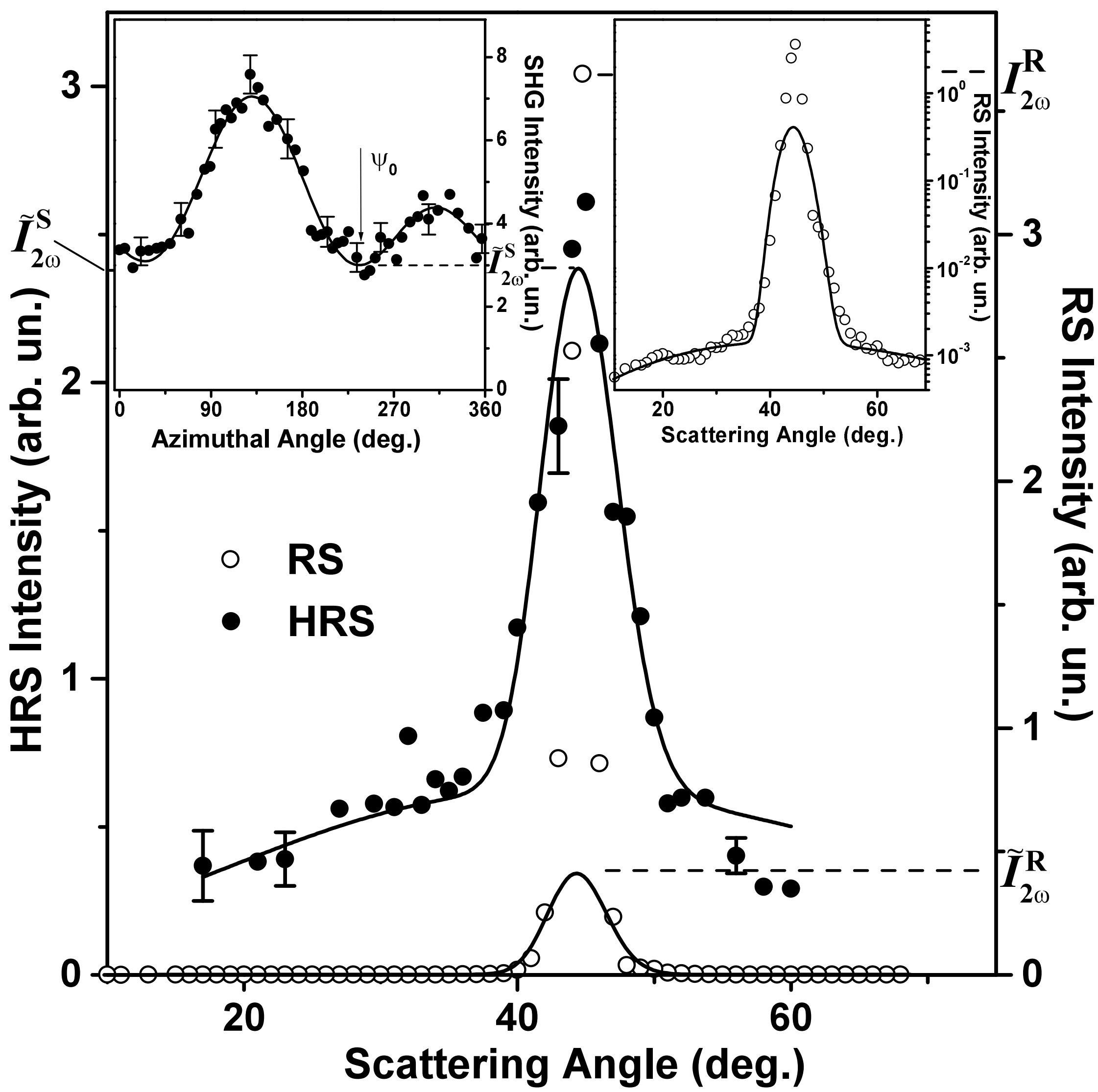

HRS Intensity (arb. un.)
RS Intensity (arb. un.)
Scattering Angle (deg.)
RS
HRS
$\tilde{I}^{S}_{2\omega}$
$I^{R}_{2\omega}$
$\tilde{I}^{R}_{2\omega}$
Azimuthal Angle (deg.)
SHG Intensity (arb. un.)
ψ_0
RS Intensity (arb. un.)
Scattering Angle (deg.)